Electronic Supplementary Material (ESI) for Soft Matter.
This journal is © The Royal Society of Chemistry 2018

Supporting Information for:

Partitioning-dependent Conversion of Polyelectrolyte Assemblies in Aqueous-Two Phase System

Qingming Ma,†‡ Hao Yuan,†‡ Yang Song,§ Youchuang Chao,†‡ Sze Yi Mak,† ‡ Ho Cheung Shum*†‡

† Department of Mechanical Engineering, University of Hong Kong, Pokfulam Road, Hong Kong, China

‡ HKU-Shenzhen Institute of Research and Innovation (HKU-SIRI), Shenzhen 518000, China

§Current address: Department of Biomedical Engineering, University of Michigan, Ann Arbor, USA

1. Partitioning-dependent fabrication of polyelectrolyte microcapsules.

Typically, the droplet and continuous phases of the aqueous emulsion are water with dextran and poly (ethylene glycol) (PEG), respectively. A solution of dextran and PEG with molecular weights of 500,000 Da and 8,000 Da respectively is known to separate into immiscible dextran-rich and PEG-rich phases when the dextran and PEG concentrations increase above 10*wt*% and 8*wt*% at pH 7.0. The polycations, FITC-PAH, is dissolved in the dextran solution and electrosprayed into the PEG solution containing the polyanions, PSS, to form the dextran-in-PEG emulsion droplets. At pH 7.0, for the combination of a dextran-rich phase containing PAH and a PEG-rich phase containing PSS, the strong partitioning-dependent distribution of PSS leads to strong inward migration of PSS from the continuous phase (PEG) to the droplet phase (dextran), while the weak partitioning-dependent distribution of PAH leads to weak outward migration of the PAH. Consequently, the counter-flow of PSS and FITC-PAH facilitates the complexation at the interface of the ATPS, thus achieving the fabrication of microcapsules with liquid cores at pH 7.0.

2. Determination of the partitioning coefficient of polyelectrolytes & nanoparticles in dextran and PEG phase.

The partitioning coefficient, which is a ratio of the concentration of a compound in the two immiscible phases of a mixture of two solvents, [1] measures the different amounts of the compound dissolved in the two liquid phases.[2] Using PSS as an example, the corresponding partitioning coefficients in the two immiscible phases of dextran-rich and PEG-rich solutions were determined as follows. Initially, a 20*wt*% dextran solution and a 16*wt*% PEG solution were mixed at a 1:1 volume ratio and left sitting until the resultant solution mixture separated into two distinct immiscible phases, with the PEG-rich phase above the dextran-rich phase. PSS was then added to the dextran-rich and PEG-rich phases separately, at different known concentrations. As PSS shows a distinct absorbance signal in the solutions at a wavelength of 248nm[3,4] under

UV-vis spectrometer, two calibration curves relating the concentration of PSS to the absorbance values in the dextran-rich and the PEG-rich phases can be obtained. For the experimental systems, a known amount of PSS was dissolved in the mixture of 20*wt*% dextran solution and 16*wt*% PEG solution at a 1:1 volume ratio before the mixture was left sitting to obtain a fully phase-separated mixture, with the PEG-rich top phase and the dextran-rich bottom phase both containing equilibrium concentration of PSS. Afterwards, equal volumes of the dextran-rich phase and the PEG-rich phase containing PSS were extracted and the absorbance values of the two solutions at 248nm were measured using a UV-vis spectrometer as the test samples. Then the concentrations of PSS partitioned to dextran-rich and PEG-rich phases can be calculated using the previously obtained calibration curves. Thus the partitioning coefficients of PSS in the dextran-rich phase and the PEG-rich phase can be determined.

PSS was used as an example to demonstrate how the partitioning coefficients were obtained experimentally. Initially, a 20*wt*% dextran solution and a 16*wt*% PEG solution were mixed at a 1:1 volume ratio and left sitting until the resultant solution mixture separated into two distinct immiscible phases, with the PEG-rich phase above the dextran-rich phase. Afterwards, equal volumes of the dextran-rich phase and the PEG-rich phase were extracted, respectively. Different known amounts of PSS were dissolved in the extracted PEG solutions. Subsequently, the absorbance of the solutions at 248nm was measured using a UV-vis spectrophotometer with the pure, extracted PEG solution as blank. The resultant calibration curve of absorbance as a function of the PSS concentration can be used to calculate the concentration of PSS in the PEG-rich phase, as shown by the plot in Figure S1.

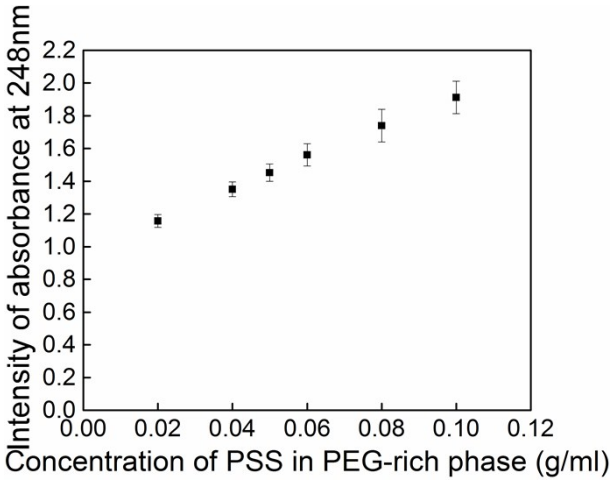

Figure S1. Calibration curve of absorbance values as a function of the PSS concentrations in PEG-rich phase.

The regression equation was $A = 9.504C_{PSS\text{-}PEG}+0.974$;

where A was absorbance value; $C_{PSS\text{-}PEG}$ was the concentration of PSS in PEG phase. Correlation coefficient R=0.999, range of concentration = 0.02-0.1 g/ml.

A calibration curve of absorbance values as a function of the PSS concentration in the dextran-rich phase was also obtained using the same procedure with the pure extracted dextran-rich solution as blank and used in subsequent measurements to calculate the concentration of PSS in the dextran-rich phase, as shown by the plot in Figure S2.

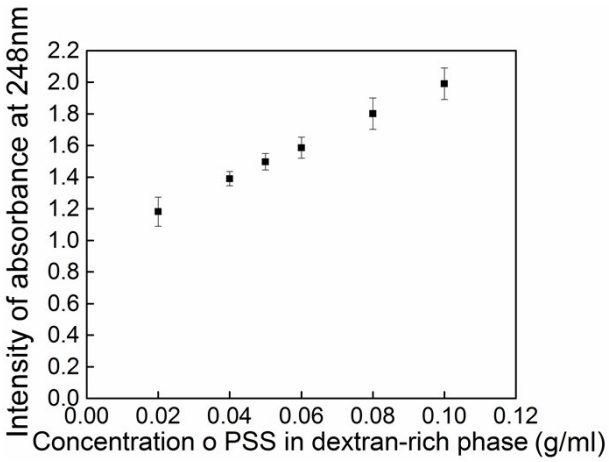

Figure S2. Calibration curve of absorbance as a function of the PSS concentrations in dextran phase.

The regression equation was $A = 10.127C_{PSS\text{-}dextran}+0.984$;

where $C_{PSS\text{-}dextran}$ was the concentration of PSS in the dextran-rich phase. Correlation coefficient R=0.999, range of concentration = 0.02-0.1 g/ml.

In the experimental systems, 0.1g PSS was dissolved in 2ml mixture of 20wt% dextran solution and 16wt% PEG solution at a 1:1 volume ratio before the mixture was left sitting to obtain a fully phase-separated mixture, with the PEG-rich top phase and the dextran-rich bottom phase both containing equilibrium concentration of PSS. Afterwards, equal volumes of the dextran-rich phase and the PEG-rich phase containing PSS were extracted and the absorbance values of the two solutions at 248nm were measured using a UV-vis spectrometer as the test samples. Then the concentrations of PSS partitioned to the dextran-rich and PEG-rich phases were calculated using the previously obtained calibration curves. Based on an absorbance value of 1.333 at 248nm in the dextran-rich solution, the concentration of PSS in the dextran-rich phase was calculated using the calibration curve as (1.333 - 0.984) / 10.127 = 0.0345 g/ml. Then the partitioning coefficient of PSS in the dextran-rich phase was determined as 0.0345 / 0.05= 0.69. Similarly, with an absorbance value of 1.121 for the tested PEG-rich solution, the corresponding concentration of PSS in the PEG-rich phase was calculated using the calibration curve as (1.121 - 0.974) / 9.504 = 0.0155 g/ml. Then the partitioning coefficient of PSS in the dextran-rich phase was determined as 0.0155 / 0.05= 0.31. The same protocols were used to obtain the partitioning coefficients of the other polyelectrolytes and amino-modified silver nanoparticles (amino-AgNPs, diameter 20nm, Aladdin Industrial Corporation, Shanghai, China). The partitioning coefficients of AgNPs in dextran-rich and PEG-rich phases at different typical pH values are listed in the following table.

Table S1. Experimentally observed partitioning coefficients of AgNPs in the dextran-rich and PEG-rich phases at different typical pH values.

pH value	Partitioning Coefficients in Dextran-rich phase	Partitioning Coefficients in PEG-rich phase
2.0	0.56	0.44
5.0	0.62	0.38
7.0	0.73	0.27
9.0	0.88	0.12

3. *Fabrication duration of PAH~PSS microcapsules with different partitioning coefficients in ATPS.*

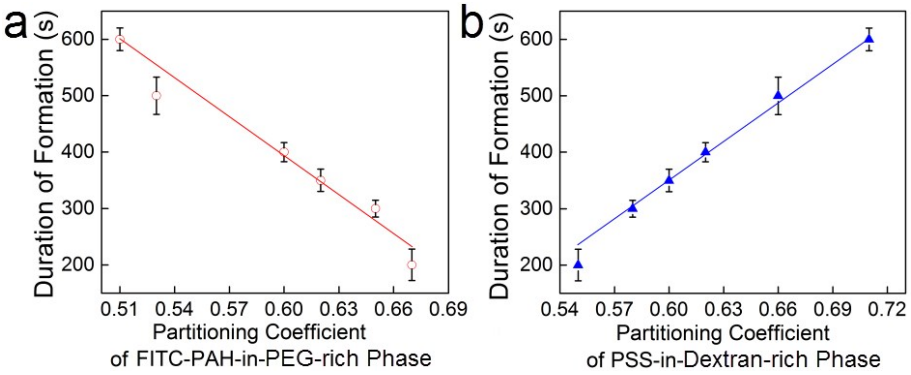

Figure S3. (a) Plots of fabrication duration of microcapsules as a function of partitioning coefficients of FITC-PAH to PEG-rich phase. (b) Plots of fabrication duration of microcapsules as a function of partitioning coefficients of PSS to dextran-rich phase.

4. *Fabrication duration of PAH~PSS microgel particles with different partitioning coefficients in ATPS.*

When increasing the pH value, the partitioning coefficient of FITC-PAH into PEG-rich phase decreases and subsequently leads to the decrease of the fabrication duration, as shown by the measured durations as a function of partitioning coefficients of FITC-PAH to PEG-rich phase in Figure S4a. On the contrary, the partitioning coefficient of PSS into dextran-rich phase increases and results in a decrease in the fabrication duration, as shown by the measured durations as a function of partitioning coefficients of PSS to dextran-rich phase in Figure S4b.

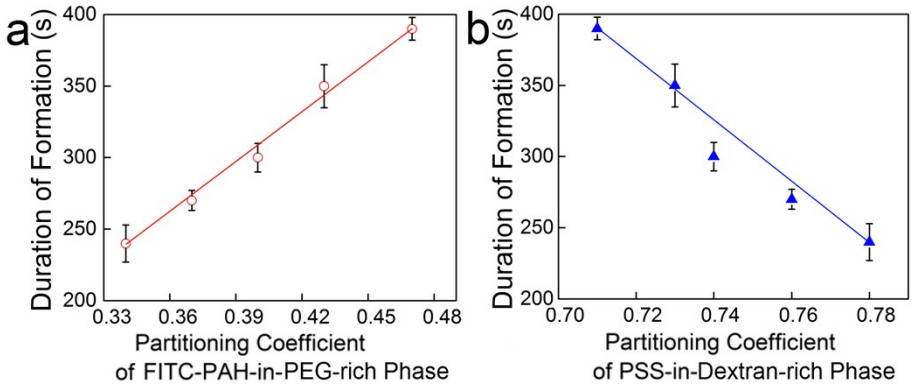

Figure S4. (a) Plots of fabrication duration of microgel particles as a function of partitioning coefficients of FITC-PAH to PEG-rich phase. (b) Plots of fabrication duration of microgel particles as a function of partitioning coefficients of PSS to dextran-rich phase.

To help explain the influence of different partitioning behaviors of the polyelectrolytes on the formation time of microgel particles, we come up with a hypothesis by considering the concentration gradient of PSS between the aqueous interface and the PEG-rich phase. Specifically, once PSS is assembled with FITC-PAH inside the dextran-rich phase to form microgel particles, a high concentration gradient of the PSS between the interface and the PEG-rich phase is created. The high concentration gradient offers a driving force for the migration of PSS from the PEG-rich phase to cross the interface and to the dextran-rich phase. Therefore, a higher partitioning of PSS towards the dextran-rich phase at higher pH value (0.79 at pH 12.0) leads to stronger inward migration of PSS from the continuous phase to the droplet phase; on the contrary, a lower partitioning of PSS towards the dextran-rich phase at lower pH value (0.71 at pH 8.0) leads to weaker inward migration of PSS[5,6]. Consequently, the diffusion of PSS from PEG-rich phase to dextran-rich phase differs at different pH values, resulting in the influence of different partitioning behaviors of the polyelectrolytes on the formation time of microgel particles.

5. *Partitioning-dependent concentration of polyelectrolytes inside one phase involved in microgel particles generation.*

Apart from the relative rates of reaction *vs* diffusion of polyelectrolytes in ATPS, the partitioning effect of polyelectrolytes in ATPS should also play an important role in the formation process of the polyelectrolyte assemblies, due to the affinity between dextran and PSS. Quantitative measurements of the reaction rates and the diffusion coefficients of all the polyelectrolytes involved are needed to get a comprehensive understanding of the mechanism of the particle formation; however, the robust measurements of them remain elusive in the current setup, and deserve a more detailed separate investigation. Moreover, it should be pointed out that asymmetric partitioning coefficients (for instance, 0.73:0.27 being the most asymmetric) do not imply the complete depletion of the polyelectrolyte from the less preferred phase. The concentrating of the FITC-PAH inside dextran-rich plays an important role at the beginning of the formation of microgel particles; however, it does not necessarily imply that all the FITC-PAH is trapped inside the dextran phase during the whole formation process.

6. *Fabrication durations of the hybrid AgNPs~PSS aggregates at different pH values.*

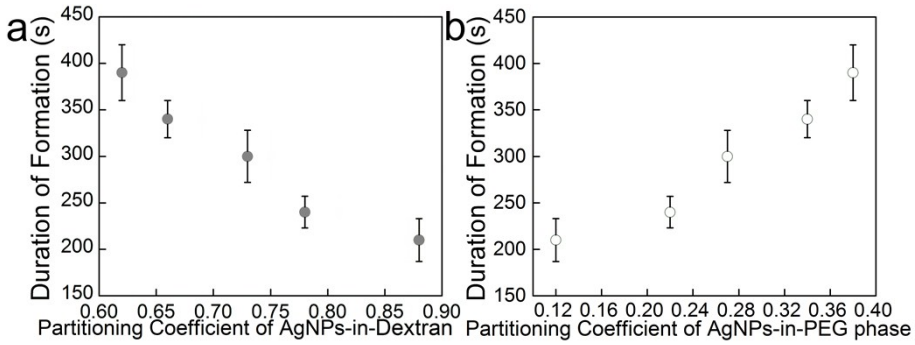

Figure S6. (a) Plots of fabrication duration of hybrid AgNPs~PSS aggregates as a function of partitioning coefficients of AgNPs to dextran-rich phase. (b) Plots of fabrication duration of hybrid AgNPs~PSS aggregates as a function of partitioning coefficients of AgNPs to PEG-rich phase.

7. *Characterization of the amino-modified silver nanoparticles.*

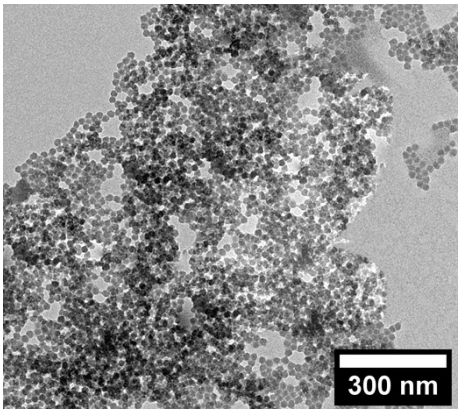

Figure S7. Transmission electron microscope image of the amino-modified silver nanoparticles with diameter of 20nm.

8. Energy-dispersive X-ray (EDX) analysis of hybrid nanoparticle-polyelectrolyte aggregates

Energy-dispersive X-ray (EDX) analysis was carried using a S-4800 FEG scanning electron microscope to confirm the presence of elemental silver signal of the silver nanoparticles assembled with PSS in the hybrid nanoparticle~polyelectrolyte aggregates.

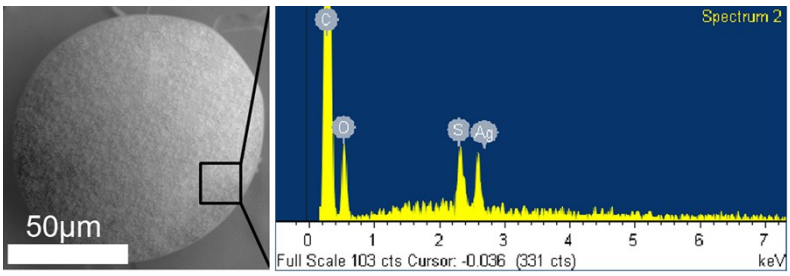

Figure S8. EDX spectrum recorded showing sharp peak between 2.5and 3 keV confirming the presence of elemental silver.

9. Microscopic imaging.

For fluorescence imaging, a confocal laser scanning microscope (Zesis LSM 700) and a fluorescence microscope (DMIL LED Fluo, Leica) were used. Optical imaging was performed using a high speed camera (Phantom v9.1) connected to an optical microscope (AE2000, Motic Inc.). All of the images were analyzed by Image J (NIH).

Reference:

(1) Leo, A.; Hansch, C.; Elkins, D. Partition Coefficients and Their Uses. *Chem. Rev.* **1971**, *71*, 525-616.

(2) Pereira, J. F. B.; Ventura, S. P. M.; e Silva, F. A.; Shahriari, S.; Freire, M. G.; Coutinho, J. A. P. Aqueous Biphasic Systems Composed of Ionic Liquids and Polymers: A Platform for the Purification of Biomolecules. *Sep. Purif. Technol.* **2013**, *113*, 83-89.

(3) Schaefer, M.; Holtkamp, J.; Gillner, A. Ablation of PEDOT/PSS with Excimer Lasers for Micro Structuring of Organic Electronic Devices. *Synth. Met.* **2011**, *161*, 1051-1057.

(4) Xiao, S.; Fernandes, S. A.; Esen, C.; Ostendorf, A. Picosecond Laser Direct Patterning of Poly(3,4-ethylene dioxythiophene)-Poly(styrene sulfonate)(PEDOT:PSS) Thin Films. *J. Laser Micro/Nanoeng.* **2011**, *6*, 249-254.

(5) J. M. Siegfried, T. G. Burke and T. R. Tritton, Cellular transport of anthracyclines by passive diffusion: Implications for drug resistance, *Biochemical pharmacology*, **1985**, *34*, 593-598.

(6) M. Arrio-Dupont, S. Cribier, G. Foucault, P. F. Devaux and A. d'Albis Mitra, Diffusion of fluorescently labeled macromolecules in cultured muscle cells, *Biophysical journal*, **1996**, *70*, 2327-2332.